

# From Antiferromagnetism to Superconductivity: Numerical Evidence for $SO(5)$ Symmetry and Superspin Multiplets

Robert Eder, Werner Hanke

Institut für Theoretische Physik, Am Hubland, D-97074 Würzburg, Federal Republic of Germany

Shou-Cheng Zhang

Department of Physics, Stanford University, Stanford, CA 94305

(March 23, 2024)

In this work, we present numerical results which support  $SO(5)$  symmetry as a concept unifying superconductivity and antiferromagnetism in the high-temperature superconductors. Using exact cluster diagonalization, we verify that the low-energy states of the  $t$ - $J$  model, a widely used microscopic model for the high  $T_c$  cuprates, form  $SO(5)$  symmetry multiplets. Our results show that the  $d$ -wave superconducting ground states away from half-filling are obtained from the higher spin states at half-filling through  $SO(5)$  rotations.

Introduction: Ever since the early days of quantum mechanics, group theoretical interpretation of spectroscopy revealed deep symmetry and profound unity of Nature. Atomic spectra can be fitted into irreducible representations (irreps) of  $SO(3)$ , and the regular patterns which emerged from this classification offered fundamental understanding of the periodic table. After the discovery of a large number of hadrons, the "embarrassment of riches" is removed by the classification of hadronic spectra into irreps of  $SU(3)$  and this hidden regularity inspired the predictions of quarks, the fundamental building block of the universe. In our quest for understanding the fundamental design of Nature, the importance of symmetry can never be over-emphasized.

In this article we report a different kind of spectroscopy, and its classification into a different kind of symmetry. The spectroscopy is performed on a computer, which numerically diagonalizes microscopic Hamiltonians, i. e. Hubbard and tight-j models widely believed [1,2] to model high- $T_c$  superconductors. One of the universal features of high- $T_c$  superconductors is the close proximity between the antiferromagnetic (AF) and the d-wave superconducting (dSC) phases [7]. While an AF insulator appears to be diagonally opposite to a superconductor, their close proximity lead one of us (SCZ) to conjecture that they are in fact intimately related by an  $SO(5)$  symmetry group which unifies them [8]. In this theory, the AF and dSC order parameters are grouped into a single five component vector  $\eta_a$  called superspin. The transition from AF to dSC is viewed as a superspin flip transition as a function of the chemical potential or doping, where the direction of the superspin changes abruptly.

While the  $SO(5)$  symmetry was originally proposed in the context of an effective field-theory description of the high- $T_c$  superconductors, its predictions can actually be tested within microscopic models. First numerical evidence for the approximate  $SO(5)$  symmetry of the Hubbard model came recently from exact diagonalizations of small-sized (10 sites) clusters [9] studying dynamic correlations functions involving the AF/dSC rotation ( $\hat{Q}$ ) operators [10,8]. In this work we shall use the tight-j model because of its more limited Hilbert space. Since the tight-j model explicitly projects out the states in the upper Hubbard band, some of the questions [11,13] raised recently about the compatibility between the Mott Hubbard gap and  $SO(5)$  symmetry can also be answered explicitly. We use a general and direct recipe for checking microscopic Hamiltonians for  $SO(5)$  symmetry, i.e. the concept of "superspin multiplets". In particular, if there is an approximate  $SO(5)$  symmetry of the microscopic model, the low-energy states of this model should fall into irreps of  $SO(5)$ . In a given quantum mechanical system, the direction of the  $SO(5)$  superspin vector is quantized in a way similar to an ordinary  $SO(3)$  spin, and the classically intuitive picture of the precession of the  $SO(5)$  superspin vector under the influence of the chemical potential [8,14] can be identified with the equal level-spacing between the members of  $SO(5)$  multiplets carrying different charge. Therefore, numerically identifying the low-lying states of the microscopic model with the  $SO(5)$  irreps can lead to detailed understanding of the one-to-one correspondence and the level crossing between the excited states of the AF and the dSC states, and thereby lead us to the microscopic mechanism by which the AF changes into the dSC state. While finite size-calculations can not generally be used to prove the existence of long range order in infinite systems, the spectroscopic information about the  $SO(5)$  symmetry can be used as input for the effective field theory [8,15,16] which captures the low energy and long distance physics of the problem.

**$SO(5)$  Superspin Multiplets, a Pyramid of Diamonnds:** The  $SO(5)$  Lie algebra is generated by ten operators  $L_{ab}$  with  $a, b = 1, \dots, 5$  and  $a < b$ . They obey the following commutation relation:

$$[L_{ab}, L_{cd}] = i(a_c L_{bd} + b_d L_{ac} - a_d L_{bc} - b_c L_{ad}) \quad (1)$$

$SO(5)$  is a rank two algebra, we can therefore choose total the charge  $Q = L_{15} = \frac{1}{2}(N_e - M)$  and z component of the total spin  $S_z = L_{23}$  to be the members of the Cartan subalgebra of mutually commuting generators. Here  $N_e$ , the number of electrons and  $M$ , the number of lattice sites are both taken to be even. Moreover, the Casimir operator  $C = \sum_{a < b} L_{ab}^2$  commutes with all generators and can be used to label the level of a representation. The operators are defined as follows

$$L_{ab} = \sum_{\mathbf{p}} g(\mathbf{p}) c_{\mathbf{p}+\mathbf{Q}}^\dagger (\delta_{ab} - \gamma_{ab}) c_{\mathbf{p}}; \quad (2)$$

where  $c_{\mathbf{p}}$  annihilates an electron with momentum  $\mathbf{p}$  (we are suppressing the spin index)  $\gamma$  is the vector of Pauli matrices, and  $\mathbf{Q} = (\pi, \pi)$  is the antiferromagnetic wave vector. If one takes  $g(\mathbf{p}) = \text{sgn}(\cos p_x - \cos p_y)$ , the  $SO(5)$  algebra closes exactly [17]. However, for cluster calculations it is often more convenient to take  $g(\mathbf{p}) = \cos p_x - \cos p_y$ , the numerical difference between these two choices is small. Together with the total spin raising and lowering operators  $S_+$ ,  $S_-$  and  $S_z$  form the root generators of  $SO(5)$  and rotate different members of a multiplet into each other.

In this paper, we are concerned with the tensorial representations of  $SO(5)$ . Tensors with given symmetry types under permutation of their indices are classified by the Young tableaux [18]. For the  $SO(5)$  group, tensors which have more than two antisymmetric indices can always be mapped to tensors with less or equal to two antisymmetric

indices by the invariant tensor  $\epsilon^{abcde}$ , the fully antisymmetric index in 5 dimensions. Therefore, all tensorial irreps of  $SO(5)$  are characterized by two integers  $(\lambda; 0)$ , corresponding to the length of two rows in the Young tableaux [18]. The general  $(\lambda; 0)$  series can only be constructed from two different  $SO(5)$  vectors. However, as we shall see later, the low lying states of the  $t$ - $J$  model can all be classified according to the restricted irreps  $(\lambda; 0)$  generated by the superspin vector alone. Therefore, we shall restrict ourselves to the fully symmetric tensors  $F_{a_1 a_2 \dots a_\lambda}$  series  $(\lambda; 0)$  generated by the products of the  $SO(5)$  vector  $n_a$ , satisfying

$$[L_{ab}; n_c] = i_{bc} n_a + i_{ac} n_b.$$

Here  $n_a$  is the five-dimensional vector  $(\sqrt{\frac{1}{2}} S_Q; i(\sqrt{\frac{1}{2}} \vec{S}_Q))$ , where  $S_Q = (\frac{1}{2})^P \sum_p c_p^\dagger c_p$  denotes the  $d_{x^2-y^2}$  superconducting order parameter and  $\vec{S}_Q = \sum_p \vec{c}_{Q+p}^\dagger \vec{c}_p$  denotes the antiferromagnetic Neel vector. However, these representations are in general not irreducible. Since  $SO(N)$  transformations preserve the norm of a vector, the pairwise trace components of  $F$  should be projected out to obtain an irreducible tensor, i.e.  $F_{a_1 a_2 \dots a_\lambda} = 0$ . Since  $F$  is symmetric, the vanishing of the first pairwise trace ensures the vanishing for all other pairwise traces. Therefore, a pairwise traceless symmetric tensor has  $\frac{N+1}{2} \frac{N+1}{2} - \frac{N+1}{2} = \frac{N(N-1)}{2}$  components, which gives the dimension

$D$  of a level  $(\lambda; 0)$  (or simply  $\lambda$ ) irreps. For  $SO(5)$  we obtain  $D = \frac{1}{6}(\lambda+1)(\lambda+2)(\lambda+3)$ , while for  $SO(3)$   $D$  reduces to the familiar degeneracy  $\lambda+1$ . The Casimir operator takes the value  $\lambda(\lambda+3)$  for a level  $\lambda$  irreps.

The linear combinations of  $n_a$ ,  $n_1 = n_5$ ,  $S_Q = n_2$ ,  $n_3$  and  $S_Q^z = n_4$  are eigenvectors of  $Q$  and  $S_z$ , and can be used to label each component of a given irrep in the two dimensional coordinate space of  $Q$  and  $S_z$ . The diagrams of the multiplets take the form of a diamond as plotted in Fig. 1. Generally, a rank  $\lambda$  irrep contains many spin multiplets, with total spin  $S = \lambda$  multiplet being the largest member. At the top of the diamond,  $Q = \lambda$  is a spin singlet, at the next sublevel,  $Q = \lambda - 1$  is a spin triplet, the  $Q = \lambda - 2$  sublevel contains both a spin singlet and a quintet. Generally, the  $Q = \lambda - p$  sublevel contains total spin  $S = p; p-2; p-4; \dots$  multiplets. These different spin multiplets takes the form of nested diamonds in a multiplet. The different diamonds at level  $\lambda$  are stacked together to form a pyramid, with  $Q = 0$  singlet at the apex, and the  $Q = M = 2$  diamond at the base of the pyramid. Each member of a given irrep is a box containing many microscopic states with the identical transformation properties under  $SO(5)$ .

**AF and dSC states in the  $SO(5)$  supermultiplet:** If we were dealing with a microscopic model with exact  $SO(5)$  symmetry [17], all the states at a given level are degenerate with each other at any finite system size. Degeneracy between different multiplets can only occur in a finite system, signaling spontaneous symmetry breaking (SSB). On a finite system, the ground state is an  $SO(5)$  singlet, lying in the  $Q = 0$  box at the apex of the  $SO(5)$  pyramid. The tendency towards SSB in the large system limit can be recognized from the scaling of the energies of excited states with higher irreps. For example, in the infinite size limit, a AF state with Neel vector in the  $xy$  plane is constructed from the linear superposition of states in the center column of the  $SO(5)$ -pyramid, while a dSC state is constructed from a linear superposition of states on the two (dSC) ridges of the  $SO(5)$ -pyramid. Because of the degeneracy within all multiplets, the AF and the dSC states constructed in the large system limit would have the same ground state energy. If one applies a chemical potential term  $H_\mu$ , the members of a given multiplet with different charge quantum numbers will be linearly shifted by the  $2Q$  term, leading to an equal level difference within a given multiplet.

In the microscopic Hubbard or the  $t$ - $J$  model used to describe the high- $T_c$  superconductors, the  $SO(5)$  symmetry is not exact, and there are different types of symmetry breaking terms. The symmetry breaking terms can also be classified according to irreducible tensors of the  $SO(5)$  Lie algebra. The chemical potential term mentioned above belongs to the 10-dimensional adjoint representation. The next simplest type of symmetry breaking term preserving spin rotation and charge conservation would be the  $Q = S_z = 0$  member of a 14 dimensional traceless and symmetric  $(2; 0)$  tensor,  $H_Q$ , transforming like  $\vec{S}_Q \cdot \vec{S}_Q$ . This type of symmetry breaking has two important effects. First it can lead to mixing of states with different quantum numbers differing by 2. The second more important effect is the removal of the degeneracy between the members of a supermultiplet carrying different charge quantum numbers. However, unlike the chemical potential term, it preserves the symmetry between the charge states with the same magnitude  $|Q|$ . This type of symmetry breaking term can remove the degeneracy between the AF and dSC states when  $\mu = 0$ , leading to a charge gap while keeping the spin excitations at low energy. However, with an applied chemical potential, the effects of these two types of symmetry breaking term can compensate each other for one type of charge states, say hole states with  $Q < 0$ , and there is a critical chemical potential  $\mu_c$  at which the multiplets with different charges  $Q < 0$  can recover their near degeneracy. As we shall see later, our overall numerical results can be consistently interpreted by these two types of explicit symmetry breaking terms. The competition between these two types of symmetry breaking terms is analogous to the competition between the spin anisotropy and an applied uniform magnetic field in an antiferromagnet, as illustrated in reference [8].

It is important to point out that, although  $H_q$  and  $H_{\text{ex}}$  can nearly compensate each other on one side of the charge states, the full  $SO(5)$  symmetry between low energy states of different signs of charge  $Q$  can not be recovered. In the  $t$ - $J$  model for example, all states with  $Q > 0$  are projected out of the Hilbert space, and the  $SO(5)$  symmetry can only be approximately realized between the members of the supermultiplets on the  $Q < 0$  half of the  $SO(5)$  pyramid. However,  $Q < 0$  states are the relevant low-energy degrees of freedom in question, and the approximate  $SO(5)$  symmetry between these states is sufficient to understand the full effect of doping. In this formalism we see the fundamental importance of the Mott-Hubbard gap (projecting out the  $Q > 0$  states) on the interplay between AF and dSC. Assuming that all the superspin multiplets are degenerate for the  $Q < 0$  states at a given  $\mu_c$ , one can either form a AF ordered state by the linear superposition of the  $Q = 0$  members of the different multiplets, or use the same coefficients to form a pure dSC ordered state by the linear superposition of the  $Q = \pm 1$  members of the different multiplets. These two states and the intermediate states between them [4] are degenerate at  $\mu_c$ . However, since a macroscopic number of  $Q < 0$  states are used to form a phase-coherent pure dSC state, it has a finite hole density. Therefore, Mott insulating behavior at half-filling is compatible with the  $SO(5)$  symmetry: AF and dSC states are nearly degenerate at  $\mu_c$ , but they have different density.

Results of exact diagonalization of the  $t$ - $J$  model: Numerical demonstration of SSB requires careful study of the level spacing as a function of system sizes, and true SSB is generally hard to establish. However, it is relatively easy to recognize a nearly degenerate multiplet structure on a finite system. For example, if we have a weakly anisotropic Heisenberg model on a lattice, the energy splitting within a multiplet would be small compared to the splitting between multiplets. Although both level spacings may scale as  $1/M$  in the limit of large system size, the ratio of their difference can be independent of the system size and its smallness thus can be recognized even with limited finite-size data. In the following, we study the  $t$ - $J$  model, the simplest model Hamiltonian which incorporates the key features of the strong-correlation limit:

$$H = P \left[ t \sum_{\langle ij \rangle} c_i^\dagger c_j + J \sum_{\langle ij \rangle} S_i \cdot S_j \right] P$$

where  $\sum_{\langle ij \rangle}$  denotes a summation over all nearest neighbor pairs on a 2D square lattice,  $P$  projects onto the subspace of states with no doubly occupied sites. The latter constraint reflects the strong correlations in the  $U \rightarrow \infty$  limit of the Hubbard model. The parameters  $t$  and  $J$  are the nearest neighbor hopping and exchange integral. We have numerically diagonalized the  $t$ - $J$  model on finite lattices of 16 and 18 sites (see Ref. [6] for pictorial representations of these standard systems) and studied its low lying eigenstates up to total spin 3 and 6 holes. In addition to their spin and charge quantum numbers, these states are also labeled by their total momentum and the point group symmetry. In figure 1 we show how some of the low lying states of the 18-site cluster  $t$ - $J$  model with  $J/t = 0.5$  split into the irreps of  $SO(5)$ , up to the  $\mathbf{10}_1 = 3$  supermultiplets. The ground states within the respective hole-number sector are labeled by an asterisk (we note that up to now this assignment of multiplets is only a conjecture; below we will present numerical evidence that these groups of states indeed are  $SO(5)$  multiplets). We see that all the different quantum numbers of the states are naturally accounted for by the quantum numbers of the superspin, and the levels with different charge  $Q$  are approximately equally spaced. More precisely, the mean level spacing within each multiplet up to  $Q = -2$  is 2.9886 with a standard deviation of 0.0769. Therefore, at a chemical potential comparable to the mean level spacing, the superspin multiplets are nearly degenerate. There are four states inside the "nested diamonds" which cannot yet be fully identified with our current methods, they are marked by the  $(\circ)$  symbol.

Now we wish to demonstrate that the different states inside a given multiplet can indeed be rotated into each other by the  $SO(5)$  root generators. In particular, we would like to show explicitly how higher spin AF states are rotated into the dSC states. Let us first briefly discuss the selection rules within figure 1. The  $S^\pm$  operators act as raising and lowering operators and obey the selection rule  $\Delta S = 0$ . In other words, they give transitions within the "diamonds" in figure 1. In the presence of an  $H_q$ -type of perturbation  $\Delta S = 2$  transitions are also possible, but are expected to have smaller amplitude. Next, as mentioned above, the 5 operators  $S^\pm$ ,  $S^z$  and  $S_Q$  together form an  $SO(5)$  vector. Consequently they play a role analogous to the dipole operator in  $SO(3)$ . They obey the selection rule  $\Delta S = \pm 1$ , i.e. they allow transitions between the different diamonds. Thereby  $S^\pm$  is a spin singlet, transfers zero momentum and has  $B_1$  symmetry, whereas  $S_Q$  is a spin triplet, transfers momentum  $(\pm 1, 0)$  and has  $A_1$  symmetry.  $S_Q$  is the operator relevant for neutron scattering, this experiment thus probes  $\Delta S = \pm 1$  transitions. As a diagnostic tool to judge if a transition from a given state  $j$  to  $i$  by the operator  $\hat{O}$  (which can be  $S^\pm$ ,  $S^z$ , or  $S_Q$ ) is possible, we compute the spectral function

$$A(\omega) = \frac{1}{\hbar} \sum_j \langle j | \hat{O}^\dagger \frac{1}{(H - E_{\text{ref}}) - i0^+} \hat{O} | j \rangle \quad (3)$$

where  $\text{Im}$  denotes the imaginary part and  $E_{\text{ref}}$  is a suitably chosen reference energy. For finite systems spectral functions of the type (3) can be calculated exactly by means of the Lanczos algorithm [6]. An intense and isolated low energy peak in (say) the  $\chi$ -spectrum (3) then indicates that there is a state with  $Q + 2$  into which  $j_i$  is being transformed by  $\chi$ . This should hold at least as long as the doped state is sufficiently low in energy to be still within the range of validity of the approximate SO(5) symmetry. Our strategy for the following, therefore, is to work ourselves through Figure 1 and to check 'SO(5)-allowed' and 'SO(5)-forbidden' transitions by computing the respective spectral functions. We can then also investigate the influence of perturbations which could possibly break the SO(5) symmetry by studying their influence on the spectra, to see e.g. how 'SO(5)-forbidden' transitions are enhanced by the perturbation.

We now begin to discuss the results of our 'computer spectroscopy'. Figure 2 compares the spin correlation function at half-filling to the spectra of the  $\chi$ -operator for the lowest 2-hole states with d-symmetry and total spin 0 and 2. The reference energy  $E_{\text{ref}}$  has been taken as the energy of the half-filled ground state. The spin correlation function has a single dominant low-energy peak at an excitation energy of  $0.5J$  (marked by an arrow) which clearly should be associated with a magnon state (all cluster states are exact eigenstates of  $S^2$  so there is no SSB in the small cluster - which explains the finite excitation energy). The spectrum of the  $\chi$ -operator for the 2 hole,  $^1B_1$  state also shows a single, high intensity peak, which coincides with that of the spin correlation function, i.e. the excitation energies agree within computer accuracy ( $10^{-13}$ ). Obviously the final states are identical, which shows that the  $\chi$ -operator indeed produces the spin resonance. Next, the spectrum of the  $\chi$ -operator for the 2 hole,  $^5B_1$  state has a strong peak at high energy, plus a low-energy peak with significantly lower intensity, which again coincides with the spin resonance. Here it should be noted that the transition from the  $^5B_1$  state with momentum  $(0;0)$  to the  $^3A_1$  state with momentum  $(\pi; \pi)$  has  $\Delta Q = 2$ , it is therefore an SO(5) forbidden transition, but it is allowed by spin, momentum or point group symmetry. Inspection shows, that the intense high energy peak in the  $^5B_1$  spectrum is nothing but the lowest  $^7A_1$  state - this  $\Delta Q = 0$  transition obviously is allowed by the SO(5) selection rule, see Figure 1. The SO(5) selection rule thus is obeyed approximately, with the ratio of the two peaks in the  $^5B_1$  spectrum being a rough measure for the degree of symmetry breaking. The pattern of the explicit symmetry breaking is consistent with that of a second rank SO(5) tensor  $H_q$ . The intensity of the peaks in the various ' $\chi$ -spectra' decreases rapidly with decreasing  $J=t$  - this indicates that corrections to the  $\chi$ -operator become more important at smaller  $J=t$ . On the other hand the additional peaks at higher energy in the ' $\chi$ -spectra' decrease rapidly as well and always stay well-separated in energy - restricting the Hilbert space to states below a cut-off frequency  $2J$  would therefore give a very good eigenoperator of the Hamiltonian.

We proceed to the 2-hole subspace, i.e.  $Q = 1$ . Figure 3 shows the spin correlation function for two holes, as well as various spectra of the  $\chi$  and  $\chi^2$  operator,  $E_{\text{ref}}$  is the energy of the two-hole ground state. To begin with, the spin correlation function again has a dominant low energy peak, whose excitation energy scales approximately with  $J$ . The final state responsible for this peak is the lowest  $^3B_1$  state with momentum  $(\pi; \pi)$ . Then, the spectrum of the operator calculated for the undoped  $^5A_1, K = (0;0)$  state, and the spectrum of the  $\chi$  operator for the  $^1A_1, K = (0;0)$  state with 4 holes also do have intense low energy peaks. These peaks are well separated from some incoherent high-energy continua, which start above a lower bound of  $2J$ , and again coincide to computer accuracy with the  $^3B_1$  state observed in the spin correlation function. This again confirms the interpretation of the spin resonance as a ' $\chi$ -excitation'. Looking at Figure 1 it becomes obvious that these two transitions have  $\Delta Q = 0$ , i.e. they are 'SO(5)-allowed'. On the other hand, the ' $\chi$ -spectrum' for the undoped ground state,  $^1A_1$ , has a weaker peak at the position of the spin resonance. This  $\Delta Q = 2$  transition is forbidden by the ideal SO(5) symmetry (see Figure 1), indicating again a weak breaking of the SO(5) symmetry. The decrease of the ' $\chi$ -peaks' with decreasing  $J=t$  is quite analogous as in the case of half-filled final states. The only exception are the peaks in the  $\chi^2$  spectra (i.e. with initial states in the 4-hole subspace), which have practically zero weight for smaller  $J=t = 0.25$ .

This also becomes clear if we study spectra with final states in the  $Q = 2$  subspace. Figure 4 shows the spin correlation function at 4 holes, together with spectra of the  $\chi$  operator for the  $^1B_1$  and  $^5B_1$  states of two holes with momentum  $(0;0)$ . From Figure 1, we see that the transition from the singlet state is forbidden, that from the quintet is allowed. Then, looking at Figure 1 it is apparent that there occurs a drastic change for  $J=t$  smaller than a cluster dependent value. For  $J=t = 0.5$  in the 18-site cluster ( $J=t = 1$  in the 16-site cluster) we have the 'standard situation': the dominant low energy ' $\chi$ -peak' for the  $^5B_1$  initial state is more intense than that for the  $^1B_1$  state, indicating again a weak breaking of the SO(5) symmetry. Both ' $\chi$ -peaks' coincide with the dominant low energy peak in the spin correlation function, which in turn stems from the lowest  $^3A_1$  state at  $(\pi; \pi)$ , which confirms that the interpretation of this peak as a ' $\chi$ -resonance' is valid throughout the low doping regime. On the other hand, for smaller  $J=t$  the correspondence between the spin correlation function and the ' $\chi$ -spectra' is essentially lost, in the case of the 16-site cluster the spin correlation function does not have a distinguishable low energy peak at all. Quite obviously, we have

reached the limit of applicability of the  $SO(5)$  symmetry, which seems to occur at a doping level of  $\sim 0.25\%$ , with some dependence on the ratio  $J=t$ . This is roughly the same parameter range where dSC correlations vanish on the finite size cluster.

Summarizing the study of the spin correlation function, we may say that the data are in overall agreement with an approximate  $SO(5)$  symmetry, in that  $SO(5)$ -allowed transitions' usually have a larger intensity than the 'forbidden' ones. The data also show that the dominant low energy spin excitation at  $(\pi, \pi)$  always can be generated by adding or removing two electrons from the system by means of the  $S^{\pm}$ -operator, which obviously supports the conjecture of Demler and Zhang [10] that this low energy resonance in the dynamical spin correlation function is the hallmark of the approximate  $SO(5)$  symmetry. The agreement with the  $SO(5)$  symmetry deteriorates for higher doping levels and/or smaller  $J=t$ .

We now proceed to map some additional transitions within the  $SO(5)$  multiplets. Figure 5 shows the spectrum of the  $S^{\pm}$ -operator for the lowest triplet state with 2 holes (this state is the one which gives rise to the prominent peak in the spin correlation function in Figure 3). The initial state thus is  ${}^3B_1(\pi, \pi)$  with 2 holes, and on the basis of Figure 1 we expect a strong transition to the  ${}^1A_1(0;0)$  state with 4 holes (i.e. the 4 hole ground state). As the reference energy we choose the energy of the 4 hole ground state, and Figure 5 then clearly shows a pronounced peak in the  $S^{\pm}$ -spectrum with zero excitation energy, precisely as expected on the basis of the  $SO(5)$  symmetry. Figures 2-5 thus demonstrate that the 4-hole ground state can be obtained by 2-fold ' $\pi$ -rotation' from the lowest  ${}^5A_1$  state with momentum  $(0;0)$  at half-filling. Similarly, the 2-hole ground state can be obtained by  $\pi$ -rotation from the lowest half-filled  ${}^3A_1$  state with momentum  $(\pi, \pi)$ .

To summarize this section, we have shown that the transitions induced by the  $S^{\pm}$  and  $S^Q$  operators can be well understood in the framework of a weakly broken  $SO(5)$  symmetry. We have explicitly identified the multiplets with  $Q = 0;1;2;3$  and shown that the  $S^{\pm}$ -operator gives transitions between the members of a multiplet with different  $Q$ . Moreover, we have verified explicitly that the spin correlation function 'operates in the same subspace' as the  $S^{\pm}$ -operator, and that the prominent low energy peaks in the dynamical spin correlation function corresponds to members of the  $SO(5)$  multiplets for all dopings  $\leq 25\%$ .

**Conclusions:** We have numerically diagonalized the low lying states of the  $t-J$  model near half-filling and found that they fit into irreps of  $SO(5)$  symmetry group. At a critical value of the chemical potential, the superspin multiplets are nearly degenerate, and therefore higher spin AF states at half-filling can be freely rotated into dSC states away from half-filling. There are clearly visible effects of  $SO(5)$  symmetry breaking, which to the lowest order can be identified with the type of a symmetric traceless rank two tensor. Our overall result suggest that the low-energy dynamics of the  $t-J$  model can be described by a quantum  $SO(5)$  nonlinear model with anisotropic couplings, and the transition from AF to dSC phase can be identified with that of a superspin flop transition [8]. It is truly remarkable that while the physical properties of AF and dSC states are intrinsically different and they are characterized by very different forms of order, there exists nevertheless a fundamental  $SO(5)$  symmetry that unifies them. The dichotomy between their apparent difference and fundamental unity is in our view a key which can unlock the mystery of the high  $T_c$  superconductivity.

We would like to thank Drs. J. Berlinsky, E. Demler, H. Fukuyama, S. Givrin, C. Henley, M. Imada, C. Kallin, H. Kohno, R. Laughlin, S. M. M. and C. Nayak for useful discussions. This work is supported by FOR SUPRA II, BM BF 05 605 W WA 6), ERB CHRX CT 940438 and the NSF under grant numbers DMR-9400372 and DMR-9522415.

**Appendix: Perturbations to the  $t-J$  model and their influence on the approximate  $SO(5)$  Symmetry**  
Recently, Baskaran and Anderson [13] raised some questions concerning the effect of the diagonal hopping and nearest neighbor Coulomb interaction on the approximate  $SO(5)$  symmetry. It is then of important to check whether these perturbations are essentially irrelevant or they could lead to a breakdown of the (approximate)  $SO(5)$  symmetry. A gain, we resort to exact diagonalization calculations to address this question. To begin with, we consider the effect of an extra 'Coulomb repulsion' between holes on nearest neighbors. More precisely, we add the term  $H_V = V \sum_{\langle i,j \rangle} n_i n_j$  to the Hamiltonian, where  $n_i$  denotes the electron density on site  $i$ . Figure 6 then compares some spectra of the  $S^{\pm}$ -operator and the zero momentum pair-operator for different values of  $V$ . The left panel shows spectra with initial states in the two-hole sector, the reference energy is that of the half-filled ground state. With this choice the excitation energies of the dominant low-energy peaks in both spectra increase with  $V$ . This is natural because the repulsion  $V$  is not operative at half-filling, but will tend to increase the energies of hole-doped states. The increase, however, is significantly less than expected, being only approximately  $0.5t$  for  $V = 2t$ . This can hardly come as a surprise, because we have  $\partial E_0 / \partial V = 4 \langle n_i n_{i+\hat{x}} \rangle$ , i.e. the nearest neighbor density correlation function of holes. The latter quantity is quite small in the physical range of parameters, so  $V$  does not have a great impact. More importantly, the difference of the excitation energies of the  $S^{\pm}$  and  $\Gamma$  operators is practically independent of  $V$ . This difference of excitation energies would give the energy required to remove a  $k = (0;0)$ , d-wave singlet pair from the system and

reinsert a  $k = (\pi, \pi)$  d-wave triplet pair. This is exactly what is done in a neutron-scattering experiment – a Cooper pair from the condensate is turned into a  $\pi$ -pair while scattering an incoming neutron. The energy difference of the peak energies in Figure 6 thus should correspond to the energy of the peak in the inelastic neutron scattering cross section, and Figure 6 clearly shows that even rather strong repulsion between the holes leaves this energy unchanged. Moreover, we note that the weight of the peaks decreases only slightly with  $V$  – the decrease is also very similar for the  $\pi$ - and  $\sigma$ -operator; this would suggest that as long as superconductivity ‘survives’ the influence of  $V$ , so does the  $\pi$ -resonance. It should also be noted that the figure actually compares an SO(5) ‘forbidden’ transition (from the half-filled  $^1A_1(0;0)$  state to the  $^3B_1(\pi, \pi)$  with two holes), and an SO(5) ‘allowed’ transition (from the  $^1A_1(0;0)$  4-hole ground state to the  $^3B_1(\pi, \pi)$  state). The ratio of intensities for both transitions is  $I=3$  and it stays so more or less independently of  $V$ . This indicates that the degree of symmetry breaking is not affected significantly by  $V$ . Next, the right-hand panel in Figure 6 compares the  $\pi$ - and  $\sigma$ -spectra calculated for the ground state with two holes – it shows similar features, in particular the difference of excitation energies is independent of  $V$ , and the weights of the peaks decrease in a very similar fashion with  $V$ .

We now consider the influence of a next-nearest neighbor hopping integral  $t'$ . We choose a  $t'$  between (1;1)-like neighbors with opposite sign as  $t$ ; for noninteracting electrons this would produce a Fermi surface similar to the LDA predictions. Figure 7 again compares the spectra of the  $\pi$ -operator and the  $\sigma$ -operator with different  $t'$  and different doping levels. The reference energy again is the ground state energy at half-filling in the left panel, which shows spectra with  $n$  states in the  $Q = 1$  subspace; in the right panel, which shows  $n$  states in the  $Q = 2$  subspace  $E_{ref}$  is the ground state energy of two holes. The overall picture is comparable to that seen in Figure 6, i.e. the difference in excitation energies is nearly independent of  $t'$ , and in fact even decreases with increasing  $t'=t$ . In the spectra with 4-hole  $n$  states this obviously leads even to a kind of level-crossing, in that the lowest  $\pi$ -peak comes down below the lowest  $\sigma$ -peak for large  $t'$ . The intensity of both low-energy peaks decreases in an essentially similar fashion with increasing  $t'=t$ . One can, however, realize a kind of ‘crossover’ between  $t'=t=0.1$  and  $t'=t=0.2$ , where the spectral weight of the  $\sigma$ -spectra drops sharply. The ultimate reason is a level crossing in the 4-hole sector from the SO(5)-compatible  $^1A_1$  ground state to a  $^1B_1$  ground state, which occurs in between these two values of  $t'=t$ . We note that 4 holes in 18 sites correspond to a hole density of 22%, which is nominally far overdoped – the drop in the  $\sigma$ -spectra thus is not really a reason for concern. Moreover, the peak in the spectrum of the  $\sigma$ -operator (which is not affected by the level crossing) stays well defined, its intensity decreasing slightly and in proportion to that of the  $\pi$ -peak. All in all it is obvious that larger values of  $t'$  degrade the SO(5) symmetry. On the other hand, practically all of our data show an intimate relationship between the d-wave pairing amplitude and the  $\pi$ -amplitude. If the  $\pi$ -resonance is suppressed, be it due to high doping, large  $V$  or large  $t'$ , so is usually the d-wave pairing. It is then only natural to conclude that as long as the d-wave pairing ‘survives’ the influence of perturbations, so does the  $\pi$ -resonance.

- 
- [1] P.W. Anderson, Science 235, 1196 (1987).
  - [2] F.C. Zhang and T.M. Rice. Phys. Rev. B 37, 3759 (1988).
  - [3] D. Scalapino, Phys. Rep. 250, 329 (1995), and in D. Scalapino, E. Loh, and J.E. Hirsch Phys. Rev. B 34, 8190 (1986), Phys. Rev. B 35, 6694 (1987)
  - [4] J.R. Schrieffer, X.G. Wen, and S.C. Zhang. Phys. Rev. B 39, 11663 (1989).
  - [5] D. Pines. Physica C 235, 113 (1994).
  - [6] E. Dagotto, Rev. Mod. Phys. 66, 63 (1994).
  - [7] V. Emery, S. Kivelson and O. Zachar, cond-mat/9610094.
  - [8] S.C. Zhang, Science 275, 1089 (1997)
  - [9] S. M. Eixner, W. Hanke, E. Demler and S.C. Zhang. cond-mat/9701217.
  - [10] E. Demler and S.C. Zhang. Phys. Rev. Lett. 75, 4126 (1995).
  - [11] M. Greiter, cond-mat/9705049.
  - [12] E. Demler et al., cond-mat/9705191.
  - [13] G. Baskaran and P.W. Anderson, cond-mat/9706076.
  - [14] E. Fradkin, Nature 387, 18 (1997).
  - [15] C. Burgess and C. Lutken, cond-mat/9705216.
  - [16] D. Arovas, J. Berlinsky, C. Kallin, and S.C. Zhang, cond-mat/9704048.
  - [17] S. Rabello, H. Kohno, E. Demler, and S.C. Zhang, cond-mat/9707027; C. Henley, unpublished.
  - [18] M. Hamermesh, "Group Theory", Addison-Wesley, (1962).

FIG. 1. The upper diagram illustrates a general level scheme of  $SO(5)$ . Every state can be labeled by  $Q$  and  $S_z$ . The maximal charge is  $Q = 1$ . The states labeled by  $a$  form the shape of a diamond, while states inside the nested diamonds are labeled by  $b$  and  $4$ . Overlapping states with same  $Q$  and  $S_z$  are distinguished by their  $S$  quantum numbers. The lower diagrams are for  $S = 1, 2, 3$  irreps of  $SO(5)$ . The figure shows the energies of some low energy states for the 18-site cluster with  $J=t = 0.5$ . The states are grouped into different multiplets and are labeled by the spin, point group symmetry, and total momentum.  $A_1$  denotes the totally symmetric,  $B_1$  the  $d_{x^2-y^2}$ -like representation of the  $C_{4v}$  symmetry group. The  $()$  symbol denotes as yet unidentified members of the respective multiplet.

FIG. 2. Comparison of spectral functions with undoped states: dynamical spin correlation function for momentum transfer  $Q$ , calculated for the half-filled  $^1A_1(0;0)$  ground state; spectrum of the  $\gamma$ -operator, calculated for the  $^1B_1(0;0)$  ground state in the  $Q = 1$  sector; spectrum of the  $\gamma$ -operator, calculated for the lowest  $^5B_1(0;0)$  state with  $Q = 1$ . Data are shown for different cluster sizes and values of the ratio  $J=t$ .

FIG. 3. Spectral functions with undoped states in the  $Q = 1$  subspace: dynamical spin correlation function for momentum transfer  $Q$ , calculated for the half-filled  $^1B_1(0;0)$  ground state; spectrum of the  $\gamma$ -operator, calculated for the  $^1A_1(0;0)$  ground state in the  $Q = 2$  sector; spectra of the  $\gamma$ -operator, calculated for the half-filled  $^1A_1(0;0)$  ground state and the lowest half-filled  $^5A_1(0;0)$  state.

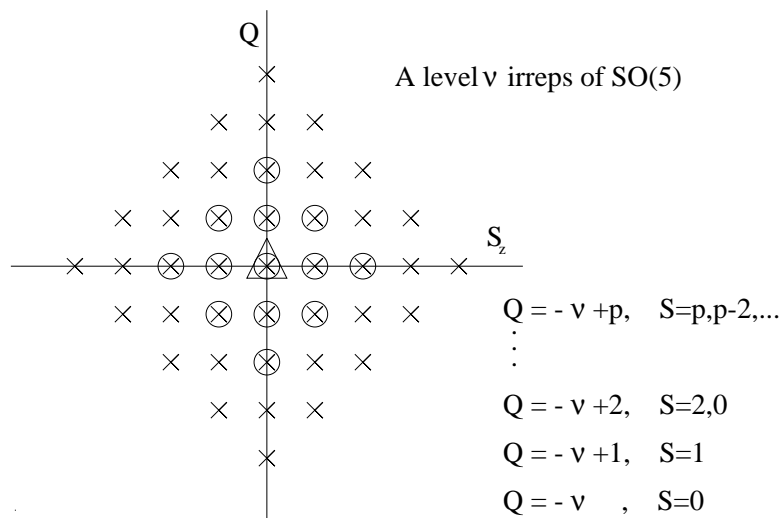
FIG. 4. Spectral functions with undoped states in the  $Q = 2$  subspace: dynamical spin correlation function for momentum transfer  $Q$ , calculated for the  $^1A_1(0;0)$  ground state; spectra of the  $\gamma$ -operator, calculated for the  $^1B_1(0;0)$  ground state and the lowest  $^5B_1(0;0)$  state in the  $Q = 1$  subspace.

FIG. 5. Spectrum of the  $\gamma$ -operator in the spin resonance state  $^3B_1(\pm; \pm)$  at  $Q = 1$ ; this state is the undoped state corresponding to the dominant peak in Figure 3.

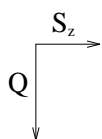
FIG. 6. Spectra of the  $\gamma$  and  $\gamma$ -operator for different  $V$ .

FIG. 7. Spectra of the  $\gamma$  and  $\gamma$ -operator for different  $t$ .  $t^0 = t$ .  $t^0$  has opposite sign as  $t$ .





$\nu=0$	0
0	0.000 ${}^1A_1(0,0)^*$



$\nu=1$	-1	0	1
0	0.2542	0.2542	0.2542 ${}^3A_1(\pi, \pi)$
-1		-2.6353	${}^1B_1(0,0)^*$

$\nu=2$	-2	-1	0	1	2
0	0.7601	0.7601	0.7601	0.7601	0.7601 ${}^5A_1(0,0)$
-1		-2.1975	-2.1975	-2.1975	${}^3B_1(\pi, \pi)$
-2			-5.2568		${}^1A_1(0,0)^*$

$\nu=3$	-3	-2	-1	0	1	2	3
0	1.5160	1.5160	1.5160	1.5160	1.5160	1.5160	1.5160 ${}^7A_1(\pi, \pi)$
-1		-1.4260	-1.4260	-1.4260	-1.4260	-1.4260	${}^5B_1(0,0)$
-2			-4.5205	-4.5205	-4.5205		${}^3A_1(\pi, \pi)$
-3				-6.6156			${}^1B_1(0,0)^*$

